REPORT NO. FRA-OR&D 75-46

HAZARDOUS MATERIALS TANK CARS- EVALUATION OF TANK CAR SHELL CONSTRUCTION MATERIAL

G. E. Hicho
C. H. Brady

SEPTEMBER 1970
FINAL REPORT

Prepared For
DEPARTMENT OF TRANSPORTATION
FEDERAL RAILROAD ADMINISTRATION
Office of Research and Development
Washington, D.C. 20590

NOTICE

This document is disseminated under the sponsorship of the Department of Transportation in the interest of information exchange. The United States Government assumes no liability for its contents or use thereof.

Technical Report Documentation Page

1. Report No.	2. Government Accession No.	3. Recipient's Catalog No.
FRA-OR&D 75-46		

4. Title and Subtitle	5. Report Date
HAZARDOUS MATERIALS TANK CARS-EVALUATION OF TANK CAR SHELL CONSTRUCTION MATERIAL	September 1975
	6. Performing Organization Code
7. Author(s)	8. Performing Organization Report No.
G.E. Hicho, C.H. Brady	312.01/14
9. Performing Organization Name and Address	10. Work Unit No. (TRAIS)
National Bureau of Standards Washington, D.C. 20234	11. Contract or Grant No. DOT-AR-10023
	13. Type of Report and Period Covered
12. Sponsoring Agency Name and Address	FINAL REPORT
U.S. Department of Transportation Federal Railroad Administration Office of Research and Development Washington, D.C. 20590	14. Sponsoring Agency Code

15. Supplementary Notes

16. Abstract

A metallurgical analysis of a steel plate sample (the Bell sample) was requested by the Federal Railroad Administration. The steel sample was taken from a tank car (number 88300) which had been involved in an accident near Bell, West Virginia. An investigation was conducted at the National Bureau of Standards to characterize the steel from the failed tank car and to determine whether the steel meets the specification AAR TC 128-69. Another purpose ot the investigation is to determine the nature of the fracture of the head plate of the failed tank car.

17. Key Words	18. Distribution Statement
Metallurgical, Tank Cars	Document is available to the public through the National Technical Information Service, Springfield, Virginia 22161

19. Security Classif. (of this report)	20. Security Classif. (of this page)	21. No. of Pages	22. Price
Unclassified	Unclassified	35	

TABLE OF CONTENTS

INTRODUCTION

"Hazardous Materials Tank Cars - Evaluation of Tank Car Shell Construction Material"

Background: Tank Car #88300 was impacted in the head plate by another railroad car and upon impact the head plate fractured. The incident occurred in Bell, West Virginia, January 21, 1970, where the ambient temperature on the day of failure was -2° F.

Material: The failed plate (identified as plate RR) was submitted to NBS by the Bureau of Railroad Safety, Federal Railroad Administration, Department of Transportation, for examination. The plate was approximately 11/16 inch thick and was reported to have been fabricated from a low carbon-high manganese steel. Figure 1 shows the steel plate (RR) in the as received condition with the fracture located along the right edge of the plate. Figure 2 shows the location of the failed plate (RR) in the damaged tank car.

Purpose: One purpose of this investigation was to characterize the steel from the failed tank car numbered 88300 and to determine whether the steel meets the Specification AAR TC128-69 for Tank Car Materials. This specification is included in the report.

Another purpose was to investigate the nature of the fracture.

Examinations: Tensile, impact, and hardness tests were conducted on the plate. Tensile and impact specimens were taken in two directions approximately 90° to each other in order to establish whether directional properties existed. A chemical analysis and a complete metallographic examination were also performed on the submitted plate. The locations of the test samples used in this investigation are shown in figure 3.

Hardness: Rockwell B hardness determinations were obtained on the plate (area A, figure 3) and are reported in Table 1. The hardness of the plate was relatively uniform with an average hardness of Rockwell B92. An investigation as to the effect of flame cutting on the hardness revealed that this effect extended to a depth of no greater than 0.1 inch. The microstructural changes (Fig. 4) that accompanied the flame cutting, occurred to a depth of approximately 0.04 inch.

Chemical Composition: A determination of the chemical composition of the steel plate was performed by the Spectrochemical and Analytical Chemistry Section of NBS. The chemical results, shown in Table 2, indicate the steel plate conforms to the AAR-TC128 Grade A Specifications. This is based on the vanadium content and low concentrations of copper, nickel, chromium, and molybdenum.

Metallographic Examination: The principal inclusions were found to be manganese sulfide. The approximate inclusion content was found from observations, at X 100, of several areas of the specimen. This inclusion content appears to be somewhat similar to those of sulfide type A, thin series 3 and 4 of figure 5 plate 1 of ASTM designation E-45.

The grain size of the steel was determined, using the ASTM grain size method, to be ASTM grain size No. 8 and finer. A photomicrograph of the grain size (which meets the requirements for this steel) is shown in figure 6. Both figures 6 and 7 show that the material has a banded structure.

An examination of the fracture surface (Fig. 8) was made to determine the nature of the fracture. A cross-sectional view of the fracture surface at low magnification is shown in figure 9. The cross section is in the area designated C_F in figure 3. Figure 9 shows that the fracture surface has a complex shape. Two sections, of the surface, designated B and C in figure 9, are approximately normal to the surface, and another section, designated A in figure 9, is approximately parallel to the surface. In section A, the fracture appears to have been predominantly brittle in nature, and in this section the fracture surface is in the plane of the bands. The microstructure adjacent to the fracture is shown in figures 10, 11, 13 and 14. In section B, which is that portion of the fracture surface nearest the outside of the plate, the fracture appears to be both brittle and ductile in nature. Evidence of brittleness was found nearest section A, and evidence of deformation was found nearest the outside surface of the plate. A similar type situation was found in section C of the fractured surface. The fracture in this section was brittle nearest section A, but evidence of deformation was found as the inside surface of the plate was approached. The deformed areas at the fractured surface, both in sections B and C, indicate that this deformation probably occurred upon impact.

A surface view of the fracture surface discussed above is shown in figure 12. Portions of section B show distinct oxidation, the oxidized portions extending into the edge of, and onto, section A. These oxidized areas indicate that over some portions of the fracture surface, a crack extending into sections B and A existed sufficiently in advance of the final fracture for oxidation to occur. Figure 12, indicates, by contrast, that section C, the inner portion of the fracture surface, was bright and rust free when received, as were some portions of section B somewhat further removed from this area of examination.

Micrographs (Figs. 15 and 16) of transverse sections of the plate, at right angles to each other, were examined in an attempt to ascertain a rolling direction. No definite conclusions could be made as to the direction of rolling from these micrographs, but further examinations indicated that the material had been cross-rolled.

Examination of the micrographs (Figs. 15 and 16) reveal that the bands consist mainly of ferrite (white areas) pearlite (black areas), and possibly some bainite (gray areas).

Banding is generally considered to be due to chemical segregation in the ingot while the molten steel is solidifying. The segregation may result from the variation of composition between the primary crystals of the dendrites and the interdendritic liquid. A light or medium degree of banding may or may not be harmful to the final product, in this case, the head plate. The banding, as present in this plate, may have some detrimental effect on the mechanical behavior of the plate, but more experimentation must be performed before a definite conclusion can be drawn.

Area G in figure 3, a section in the vicinity of the welded stiffener plate, was examined. No weld material was seen but a heat affected zone was observed. Figure 17 (a) shows, at low magnification, the heat affected zone at the outside surface of the plate in the vicinity of the welded stiffener plate. Micrograph 17 (b), shows the change between the heat affected zone (dark area) and the parent material (light area). Micrograph 17 (c), reveals the microstructure of the heated zone to be mostly bainitic. The bainite appears to be a transformation product produced during the welding operation.

Another plate, made according to the Specification AAR-TC128 Grade B, was sent to the Engineering Metallurgy Section of NBS for examination. An area of this plate was observed metallographically and the material was found to be free of the banding which had been observed in the failed head plate material. Chemical analysis by the producer showed the steel to be within Grade B Specifications.

Tensile Tests: Four tensile specimens with 0.252 inch diameter and 1 inch gage length were machined from the failed plate at the areas designated 1, 2, 3 and 4 in figure 3. The specimens were tested using a 6000 pound range testing machine. The strain rate was 0.01 inch per minute during the initial loading of the specimens, and at a load of 3600 pounds, subsequent to yielding, the strain rate was changed to 0.05 inch per minute. The tensile data are reported in Table 3.

Section M128.05 of the general AAR Specifications for Tank Cars AAR-TC128-69 requires a tensile strength of 81,000 psi to 101,000 psi, a yield strength of 50,000 psi minimum, and a minimum elongation in two inches of 19 percent. No reference is made in the specification as to the minimum amount of reduction of area that should be present in the plate. However, NBS did obtain values for the reduction of area.

The producer of the steel for the plate reports the plate to have been cold formed to ellipsoidal shape. The tensile properties were reported to be: tensile strength, 89,700 psi; yield strength, 67,300 psi; and an elongation in eight inches of 19 percent.

The results of NBS tensile tests, as shown in Table 3, indicate the plate to have tensile properties which are directional. The specimens, numbered one and two, whose axial direction was approximately the horizontal direction of the plate as welded in the tank car (see Fig. 3), had yield strength values somewhat lower than the minimum requirement of 50,000 psi. However, the yield strength values for specimens numbered three and four (see Fig. 3), whose axial direction was approximately the vertical direction of the plate as welded in the tank car, were slightly greater than the minimum required. The average value of

the yield strength for the four specimens meets the minimum requirement. The tensile strength and elongation values for all four specimens meet the specified range and minimum values respectively. The tensile strength values were near the lower limit of the required range. The average elongation value of 30.9 percent in a one inch gage length of the 0.252 inch diameter specimen indicates that the elongation in a two inch gage length of a standard 0.505 inch diameter specimen would be considerably higher than the specified amount of 19 percent.

Impact Results: Impact specimens were machined from areas A1, B1, C1, and D1 as indicated in figure 3. The impact specimens were Charpy V-notch and were made to ASTM Specification E 23-66. AAR-TC128-69 Specification, Section M128.01, states "the material shall be furnished in the as rolled condition. When specified for low temperature service the material shall be furnished normalized to meet requirements of ASTM Specification A300-68, Class 1, except that impact specimens shall be Type A Charpy V-notch as shown in ASTM Specification A370-67 and meet impact requirements at the temperature specified in the tank car specification." Type A Charpy V-notch specimen is the same in both ASTM Specifications E23-66 and A370-67. A300-68 states that the notched bar impact properties of a normalized material shall not be less than 15 ft-lb when tested at the specified temperature. The test temperature for Class 1 is -50° F. For the as rolled plate, the impact test value shall be the average of three specimens taken from each plate as rolled with not more than one value below the specified minimum value of 15 ft-lb, but in no case below 10 ft-lb. In order to fully characterize the impact properties of this material, Charpy V-notch specimens were broken at a series of temperatures from liquid nitrogen temperatures (-320° F) to +212° F. Because of lack of sufficient material, only two specimens were broken at each temperature. The notch orientation of the impact specimens is shown in figure 3. From these tests, impact curves plotting both percent energy absorbed and brittle fracture versus test temperature were determined. These results are shown in figures 18 to 25. The transition temperatures were determined from these impact curves.

The transition temperature, T_E, as used in this report, is that temperature where the energy absorbed starts to decrease abruptly with a decrease in test temperature. Similarly, at this transition temperature, there is generally an abrupt change from a completely ductile to a partially brittle appearance in the fracture.

Specimens in which the crack plane was parallel to the surface would have required specimens whose length was limited to the thickness of the plate. These specimens were not made because they could not be tested on the equipment used for the other specimens. The orientation of the test specimens in the plate with reference to the actual crack are shown in Table 4.

The impact results at the transition temperatures and at three distinct percentages of brittle fracture are shown in Table 5. Transition temperatures, TT_E, as defined above, are shown in the first column.

Specimens made from group A1 had a crack propagation direction perpendicular to the plate. The crack plane of these impact specimens was approximately parallel to the average plane of the plate fracture (Fig. 3). The specimens of this group had a transition temperature of -10° F and an energy-absorbed value of 57 ft-lb. Specimens of group C1 had their crack propagation direction through the plate, as did group A1, but their crack plane was approximately perpendicular to the plate fracture. The impact results of this group show the transition temperature to be -30° F with an energy-absorbed value of 115 ft-lb.

Specimens in groups B1 and D1, with their notch orientation normal to the surface have a crack propagation direction parallel to the surface. The crack plane of group B1 was approximately parallel and that of group D1 was approximately perpendicular to the fracture plane of the plate. There was no significant difference in the TT_E in both groups of these specimens. Group D1 specimens had higher energy-absorbed values at TT_E than group B1. Group C1 specimens had a higher energy-absorbed values at TT_E than group A1.

The impact values for groups B1 and D1 at -50° F as obtained from the curves, figures 21 and 25, indicate the impact strength of these specimens to be slightly below the required specification. Since these specimens were taken from the plate, which had been cold formed, it is possible that the impact properties in the as rolled plate would have met the specifications.

In order to check these results, and because at -50° F the impact properties are changing rapidly with temperature, sets of impact specimens were tested at -50° F as required by ASTM A300-68. These sets were designated J and K. Set J were taken from the area labeled 4 in figure 3, and set K were taken from the area labeled 7 in figure 3. Although cut from different portions of the plate, set J had a notch orientation similar to group B1 (crack plane approximately parallel to the fracture surface) and set K had a notch orientation similar to group D1 (crack plane approximately perpendicular to the fracture surface).

The results are shown in Table 6. The sets J had impact strengths of 13.0 and 13.5 ft-lb. This is similar to the results obtained from the impact strength versus temperature curves. As stated above this is less than the value of 15 ft-lb required by ASTM A300-68, but the difference can probably be accounted for by the fact that the plate had been formed, and ASTM A300-68 requires the tests to be carried out on the plate "as-rolled". However, the sets K had impact values of 4.8 and 5.5 ft-lb. This is significantly lower than the 15 ft-lb required by ASTM A300-68. To determine if this decrease in impact strength could be accounted for by the cold-forming sustained by this plate would require further investigation.

The banded structure would cause some directionality in the impact properties of the material. The fact that specimens from group A1 have different properties from those in C1, and those from B1 have different properties from those in D1 indicates that in addition to the anisotropy caused by the banded structure, the plate has an anisotropy introduced during the rolling and/or forming operations.

If tests could have been made on a group of similar size impact specimens in which the crack plane would be parallel to the section surface of the plate, it is reasonable to presume that the impact strength probably would have been much lower than those of the groups actually observed.

Conclusions: The results of the observations indicated that a crack existed in the material for some time prior to failure. At impact, the crack extended to failure. The crack was mainly brittle with appreciable areas of ductile fracture present near the inner and outer surfaces of the plate.

The exact mechanism associated with the origin of the crack could not be observed in the material since the crack origin was not available for investigation. The crack origin is thought to have been adjacent to the weld, although it is possible that the crack may have been formed during the forming operation.

The material was found to have tensile properties within the limits given in the specifications. The impact results indicate that the plate has impact properties that are directional. Part of this directionality is due to the banded structure of the plate material, and part of it is due to the rolling and/or forming process. Directionality usually occurs in a rolled steel: however directionality is accentuated by banding.

The impact results indicate that the material has directional properties, but this is not unusual. Impact results of -50° F for a set of specimens with a crack propagation plane parallel to the fracture surface were only slightly less than required by ASTM A300-68. For a set of specimens with a crack propagation direction perpendicular to the fracture surface, the impact strength was significantly lower than required by ASTM A300-68.

The chemistry results indicate the steel to contain vanadium. The presence of vanadium places the steel plate within the AAR-TC128 Grade A Specification.

Table 1. Hardness determinations on steel plate from tank car. Determinations were taken at 1/16 inch intervals from the flame cut edge of the steel plate.

Interval	Hardness R_B	Interval	Hardness R_B
1	89	10	92
2	91	11	92
3	93	12	92
4	92	13	91
5	92	14	92
6	92	15	92
7	91	16	92
8	92	17	91
9	92	18	91

Average value, R_B 92.

Table 2. Chemical composition of the tank car plate.[a] (All values in percent by weight.)

		Specification AAR-TC128 Grade A	Specification AAR-TC128 Grade B	NBS Determinations	Producers Determinations
Carbon	Max.	0.25	0.25	0.26	0.23
Manganese	Max.	1.35	1.35	1.20	1.16
Phosphorus	Max.	0.040	0.040	0.030	0.023
Sulfur	Max.	0.050	0.050	0.023	0.017
Silicon	Max.	0.30	0.30	0.21	0.23
Vanadium	Min.	.02	-	0.04	0.045
Copper	Max.	-	0.35	< 0.07	(b)
Nickel	Max.	-	0.25	< 0.05	(b)
Chromium	Max.	-	0.25	< 0.20	(b)
Molybdenum	Max.	-	0.08	< 0.06	(b)

(a) Producers heat number is 18-0682 for this steel plate.

(b) Not reported,

(-) These elements are reported only when requested by the purchaser.

Table 3. Tensile properties of the plate.

Specimen No.(a)	Tensile Strength, psi	Yield Strength (b) psi	Elongation (c) %	Reduction of Area %
1	84,500	46,000	33.1	61.7
2	84,200	48,500	32.7	64.3
3	85,100	52,700	29.5	55.0
4	85,100	54,300	28.1	53.1
Average	84,700	50,400	30.9	58.5

(a) See figure 3 for location and axial direction of tensile specimens.

(b) Yield strength at 0.2 percent offset.

(c) Elongation in one inch gage length.

Table 4. The orientation of the impact test specimens in the plate with reference to the actual crack.

Specimen Group	Specimen Axis	Notch Orientation	Specimen Crack Plane
A1	$\perp$ to crack	In surface	Approximately $\parallel$ to crack
B1	$\perp$ to crack	Normal to surface	Approximately $\parallel$ to crack
C1	$\parallel$ to crack	In surface	Approximately $\perp$ to crack
D1	$\parallel$ to crack	Normal to surface	Approximately $\perp$ to crack

Table 5. Transition temperatures (TT_E) and associated energy-absorbed values along with temperatures and energy-absorbed values at selected percentages of brittle fracture.

Impact Groups	At Transition Temperature (TT_E)		At First Sign of Brittle Fracture		At 50% Brittle Fracture		At 100% Brittle Fracture	
	TT_E	Energy Absorbed	Temp.	Energy Absorbed	Temp.	Energy Absorbed	Temp.	Energy Absorbed
	°F	Ft-lb	°F	Ft-lb	°F	Ft-lb	°F	Ft-lb
A1	-10	57	+30	40	-32	38	-80	11
B1	+45	40	+50	40	-22	24	-90	5
C1	-30	115	-15	118	-35	105	-80	13
D1	+50	61	+40	60	-12	28	-70	7

Table 6. Impact results at -50° F

Base of notch normal to plate surface

Set J: Crack plane approximately parallel to fracture.

Set K: Crack plane approximately perpendicular to fracture.

Run #1	J1	13.5 ft-lb	Average 13.0 ft-lb
	J2	17.0 ft-lb	
	J3	8.5 ft-lb	
Run #2 (Retest)	J4	11.5 ft-lb	Average 13.5 ft-lb
	J5	17.5 ft-lb	
	J6	11.5 ft-lb	
Run #1	K1	4.0 ft-lb	Average 4.8 ft-lb
	K2	4.0 ft-lb	
	K3	6.5 ft-lb	
Run #2 (Retest)	K4	6.5 ft-lb	Average 5.5 ft-lb
	K5	6.5 ft-lb	
	K6	3.5 ft-lb	

Figure 1. Photograph of the inside of a section of failed tank car plate in the as received condition. Fracture is located at right edge of photograph. X 1/3

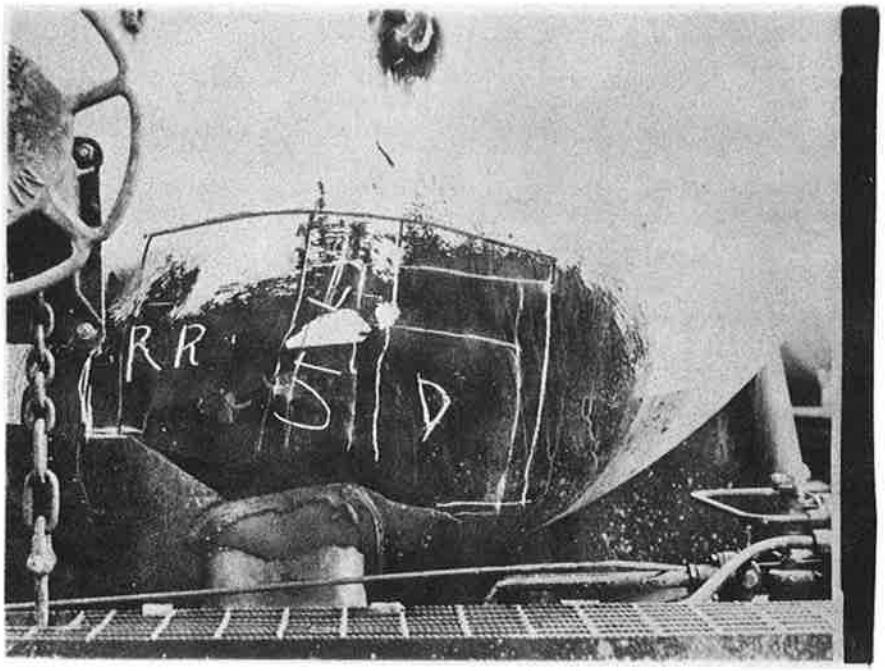

Figure 2. Location of the submitted head plate portion "RR" in the damaged tank car.

Figure 3. Photograph of the failed plate showing the areas which were used for tensile, impact, and chemical examinations. The metallographic examinations were performed on areas A, B, C_1, C_2, C_F, D, E, F and G; the hardness tests were also performed on area A. X 1/3

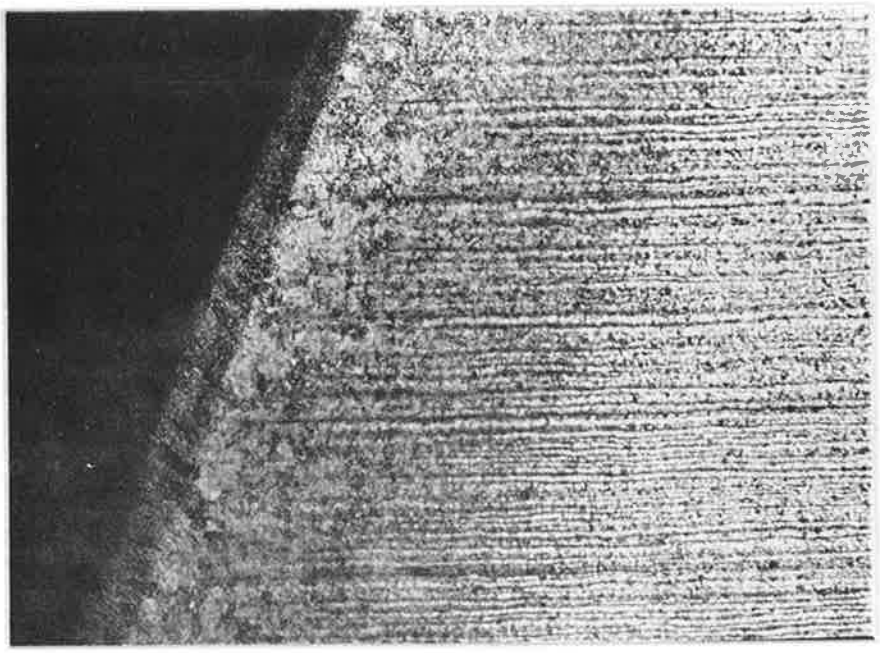

Figure 4. Photomicrograph showing the effect of flame cutting on the structure of the plate. Picral etch. X 50

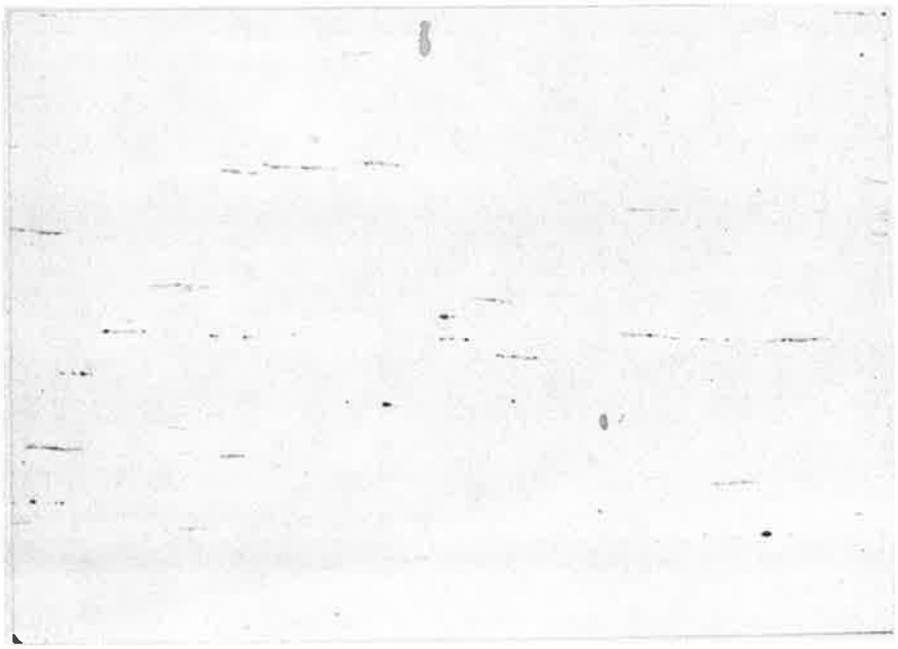

Figure 5. Photomicrograph showing the sulfide inclusions in the plate. As polished. X 100

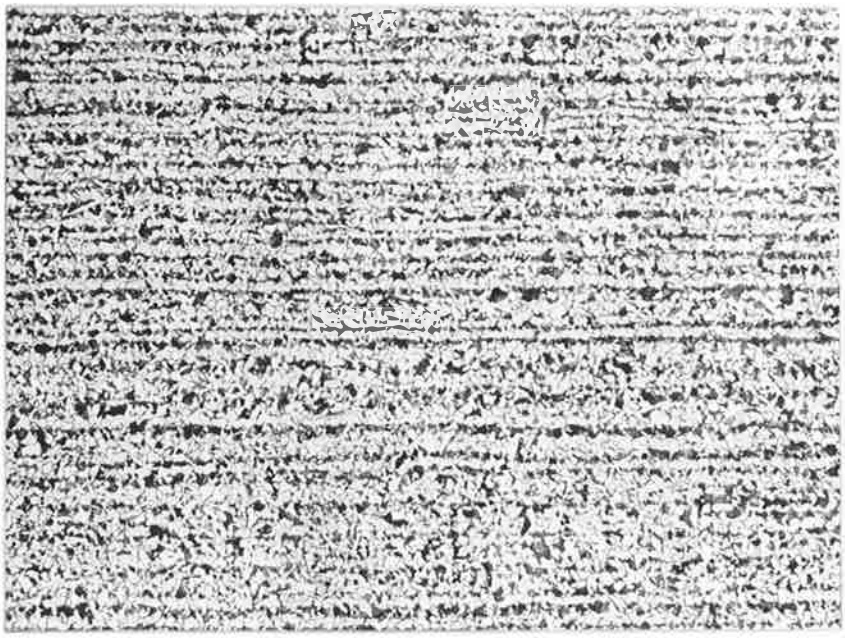

Figure 6. Photomicrograph of the banded structure of the plate. Picral etch. X 100

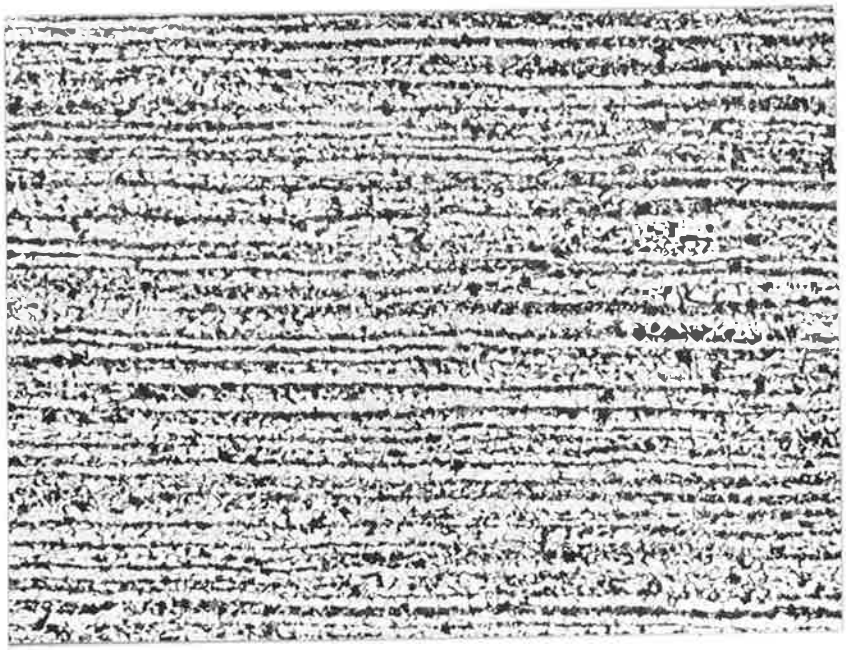

Figure 7. Photomicrograph of the banded structure of the plate. This photomicrograph was taken at about 90° to the photomicrograph shown in Figure 6. Picral etch. X 100

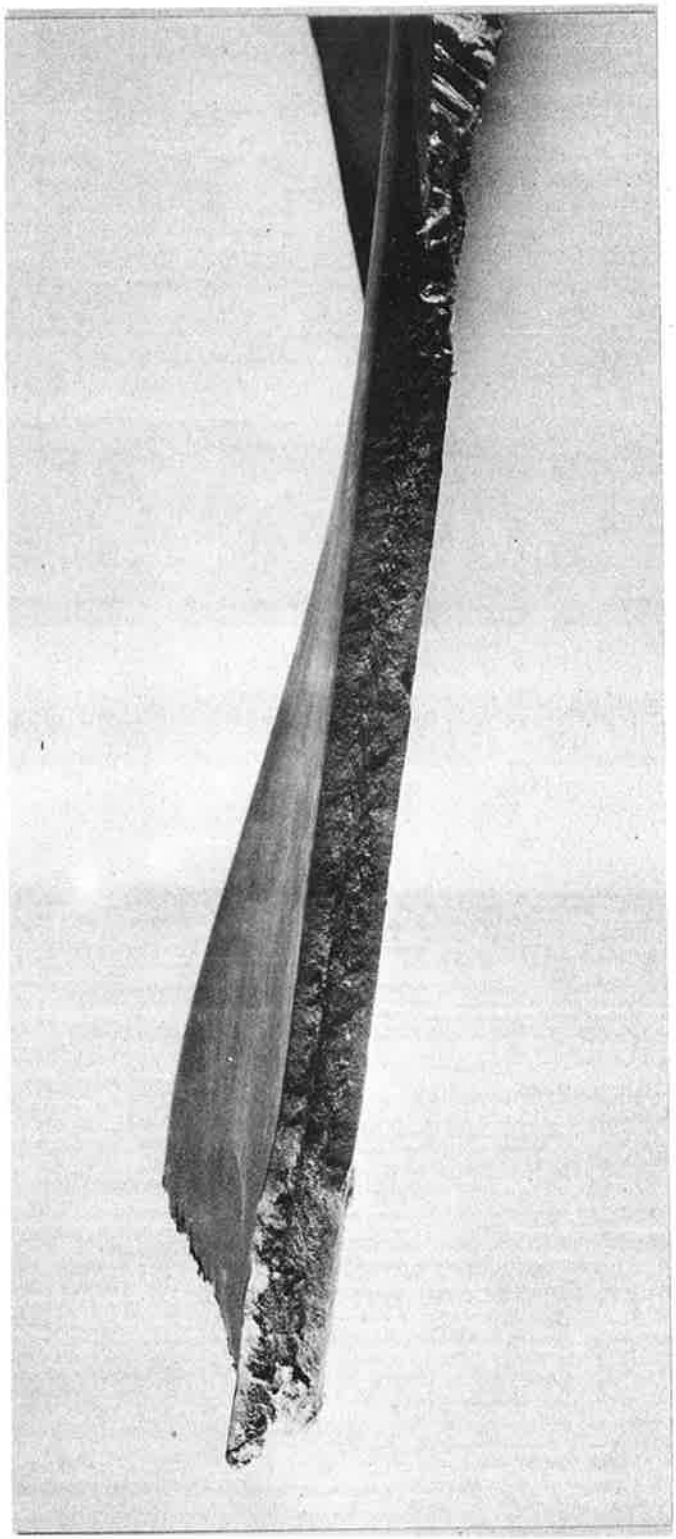

Figure 8. Photograph of the plate showing the fracture surface. X 1/2

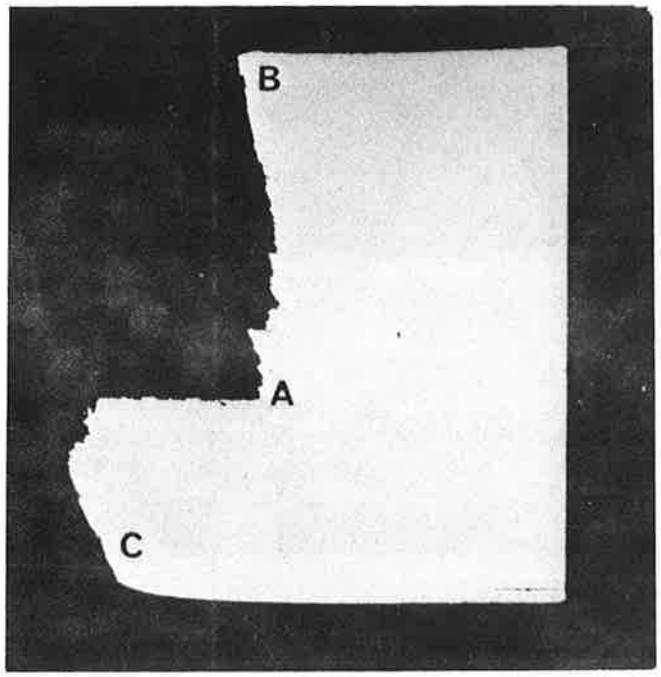

Figure 9. A thickness profile of the fracture area shown in Figure 12. A, brittle crack region; B, the outside surface of the plate; C, the inside surface of the plate.

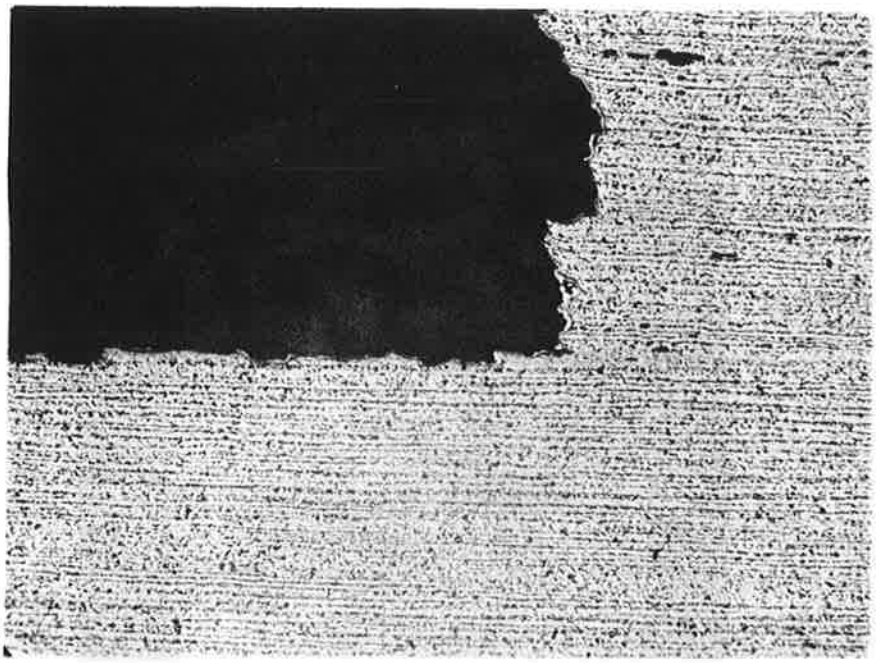

Figure 10. Microstructure at central section of the fracture (Area A, Figure 9). Part of fracture is parallel to the banded structure. Picral etch. X 40

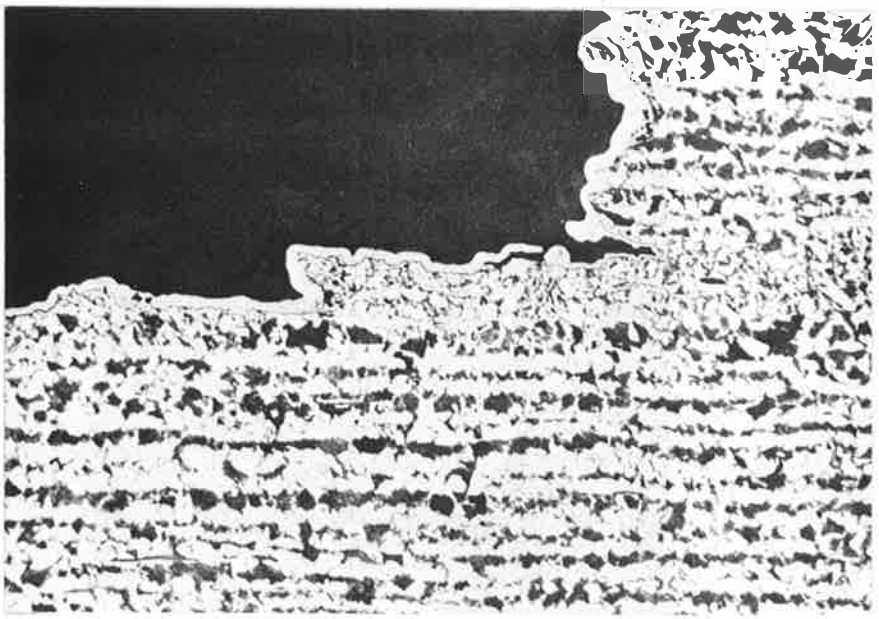

Figure 11. Microstructure adjacent to fracture path parallel to banded structure. Picral etch. X 240

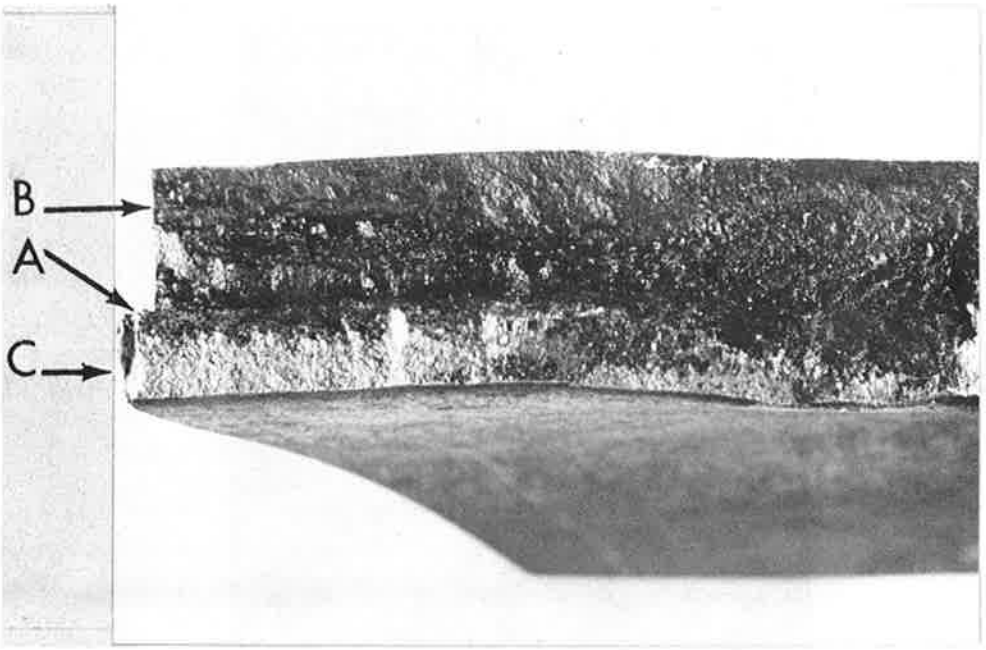

Figure 12. Photograph of a part of the fracture surface. A, brittle crack region; B, outside surface of plate; C, inside surface of the plate. Dark areas are layers of oxide (rust). Lighter areas relatively free of rust. X 1 2/3

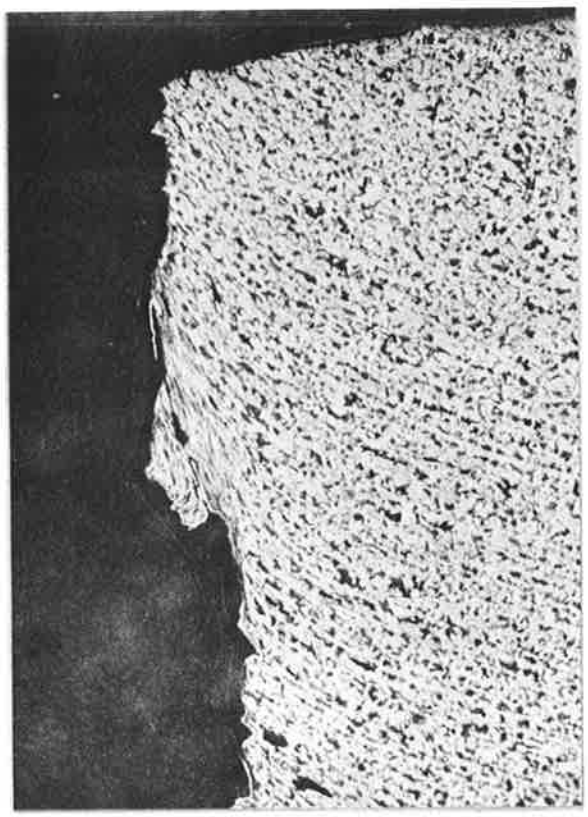

Figure 13. Microstructure at outside edge of the fracture (same area as Section B, Figure 12). Picral etch. X 100

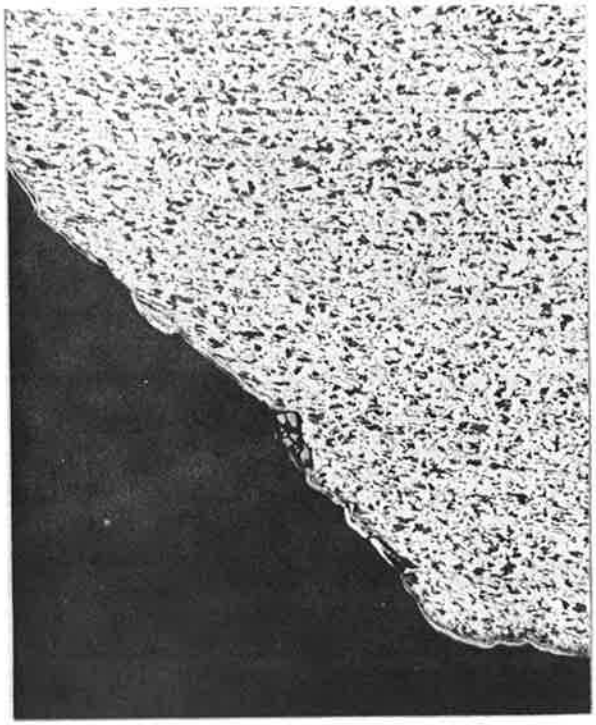

Figure 14. Microstructure at inside edge of the fracture (same area as Section C, Figure 12). Picral etch. X 100

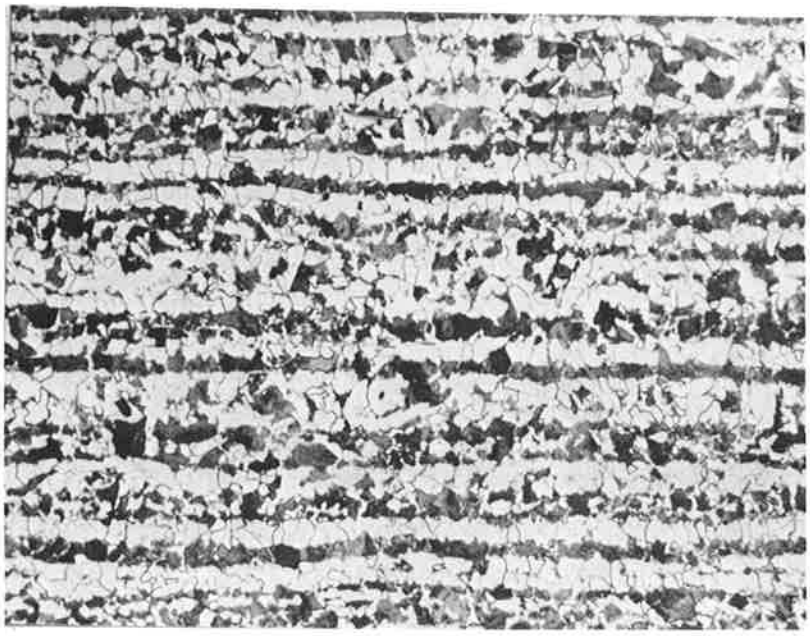

Figure 15. Photomicrograph of the banded structure. Pearlitic structure (dark areas), possible a bainitic or martensitic structure (gray areas), and ferrite (white areas). Picral etch. X 240

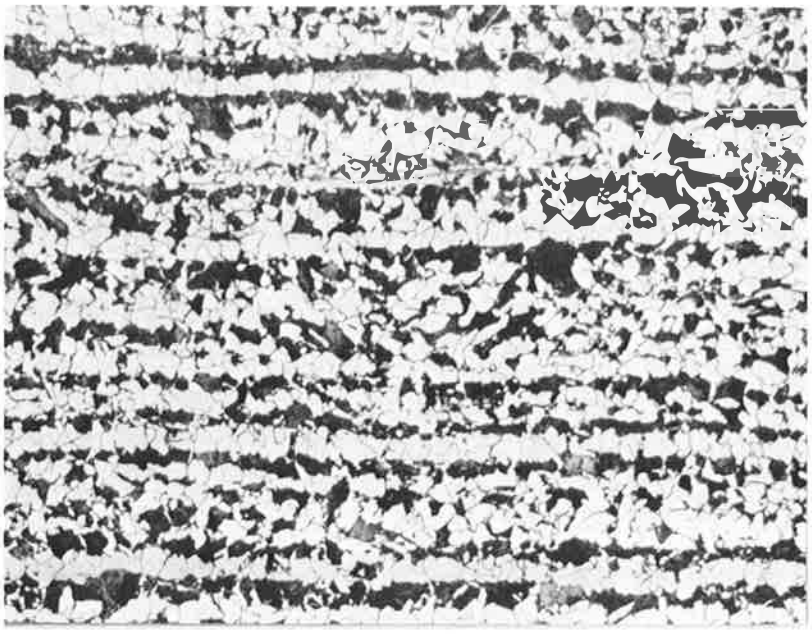

Figure 16. Photomicrograph taken at 90° to the area shown in Figure 15. Picral etch. X 240

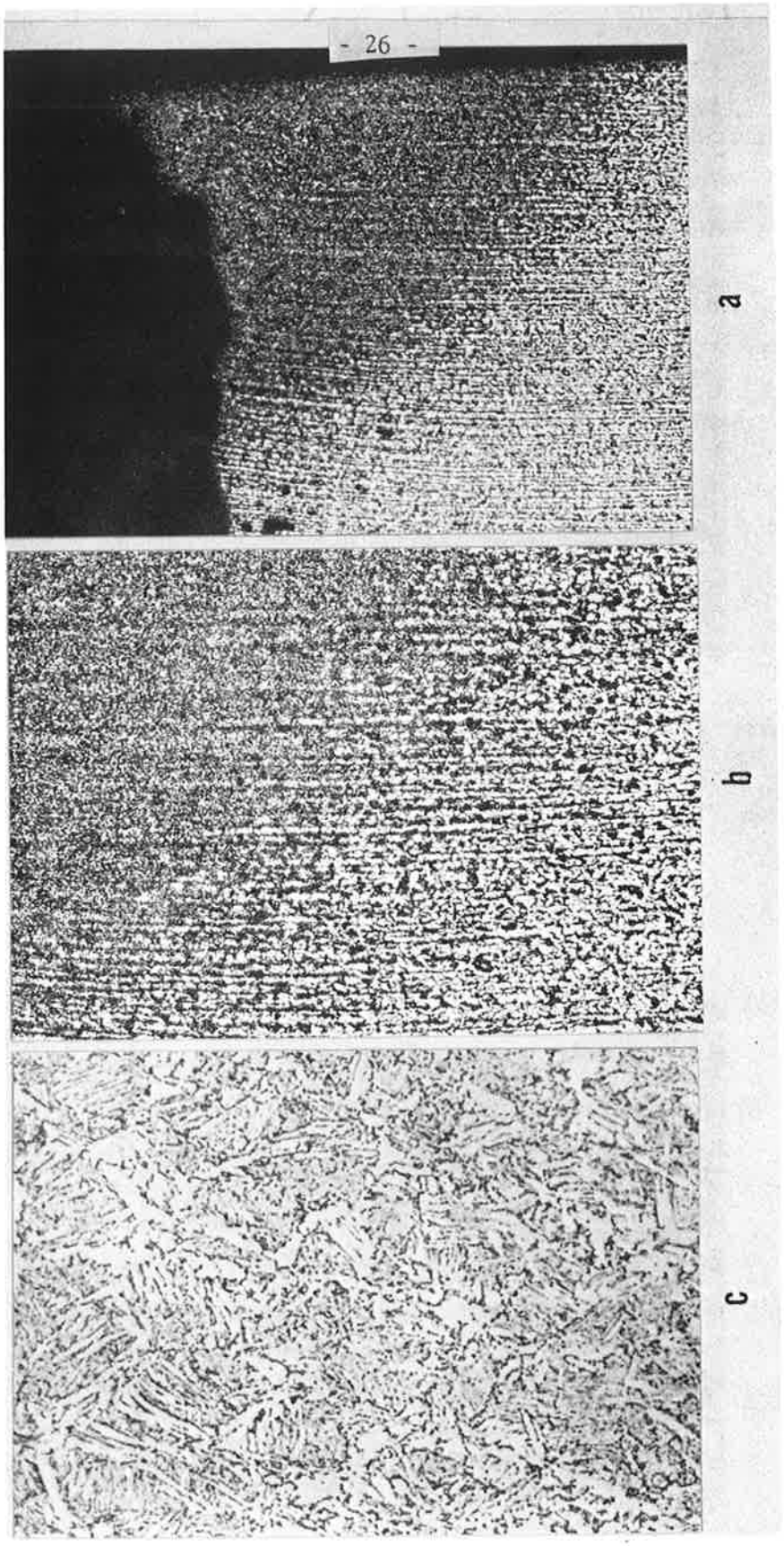

Figure 17. Photographs of an area near the outer surface and in the vicinity of the welded stiffener plate (area G, figure 3). Micrographs a, X 50, and b, X 100 show the heat affected zone and the parent material. Micrograph c, X 1200, of the heated zone reveals the bainitic structure. Picral etch.

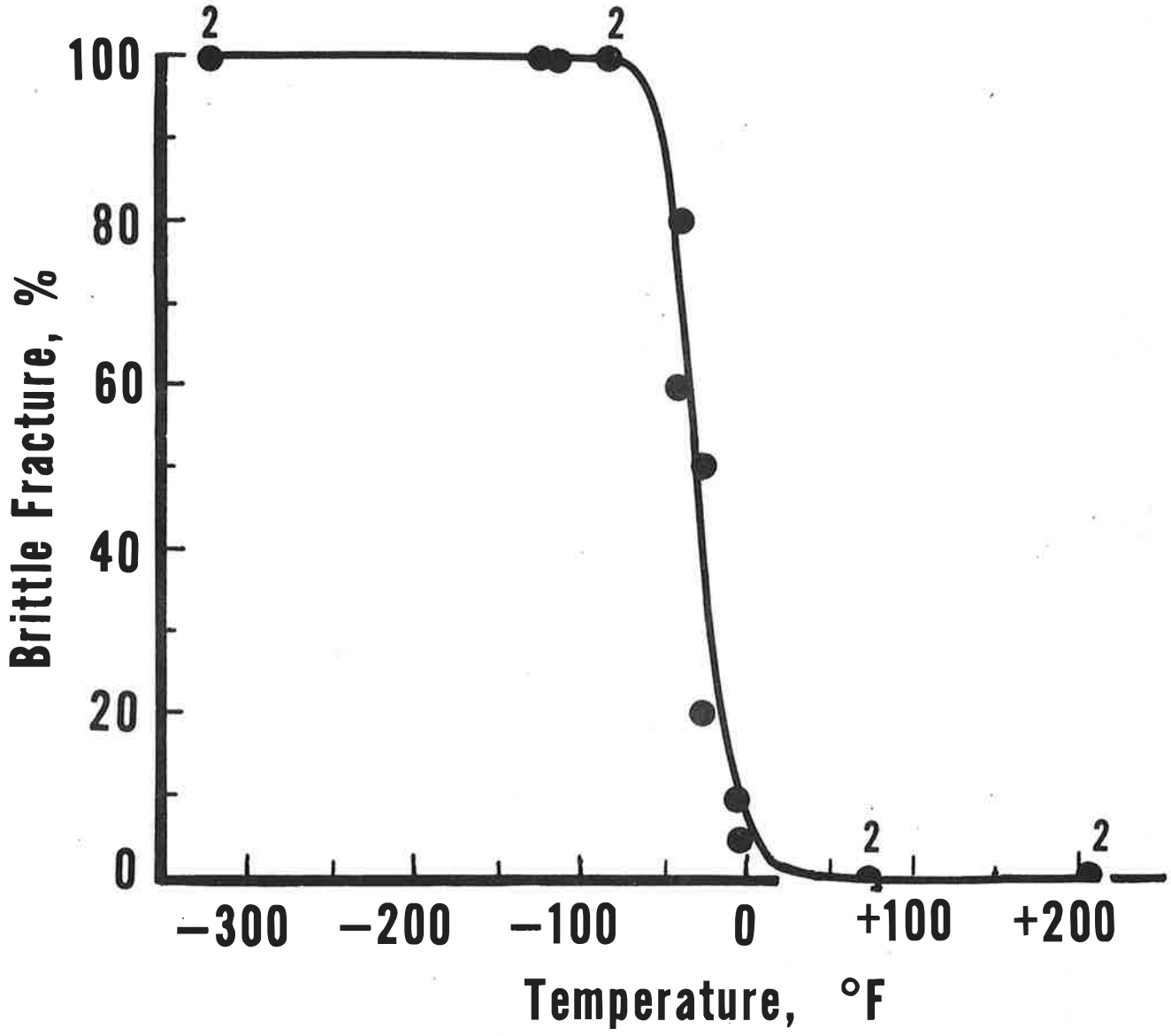

Figure 18. Effect of test temperature on the percentage of brittle fracture area of Group A1 impact specimens.

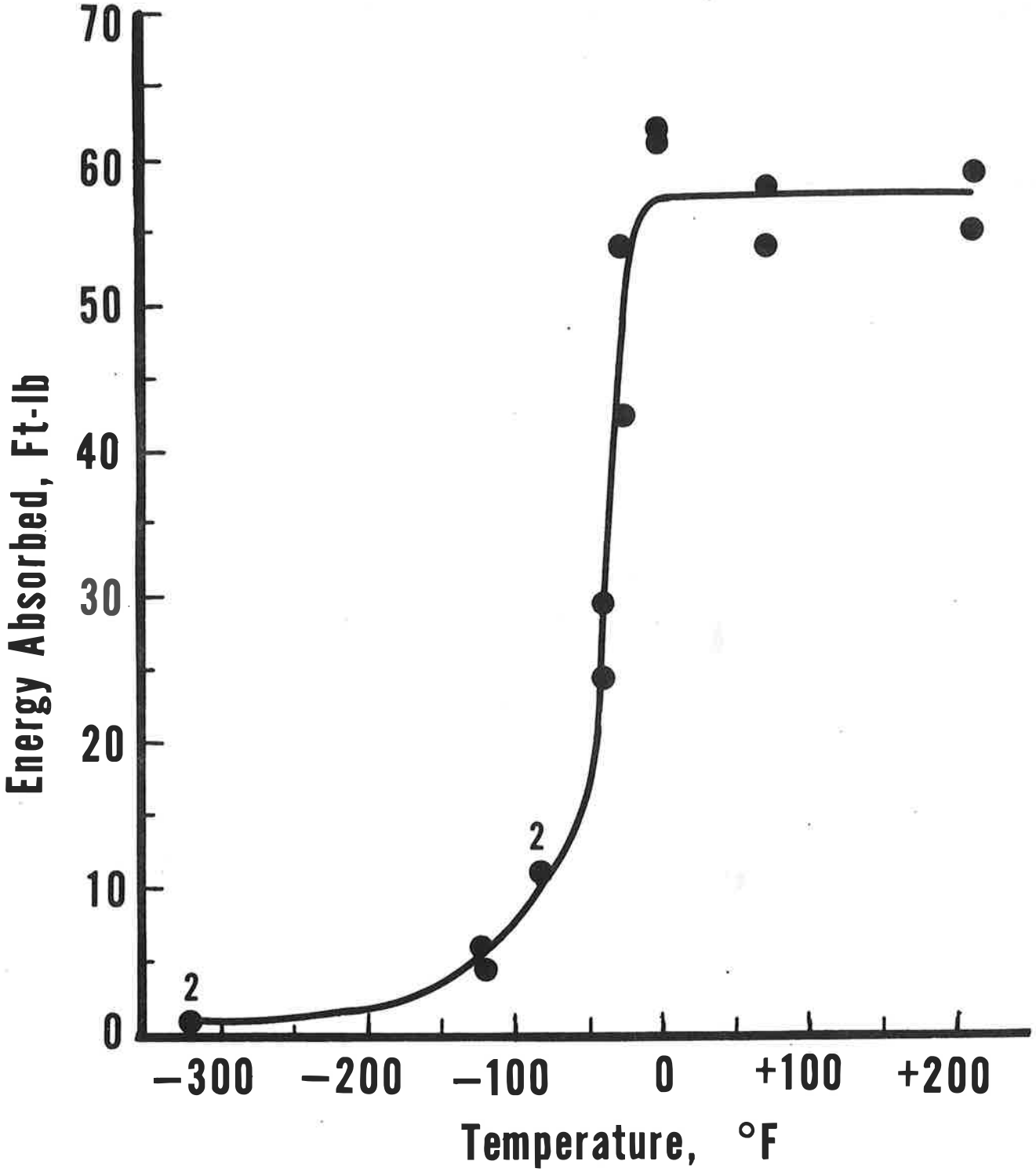

Figure 19. Effect of test temperature on the energy absorbed during fracture of Group A1 impact specimens.

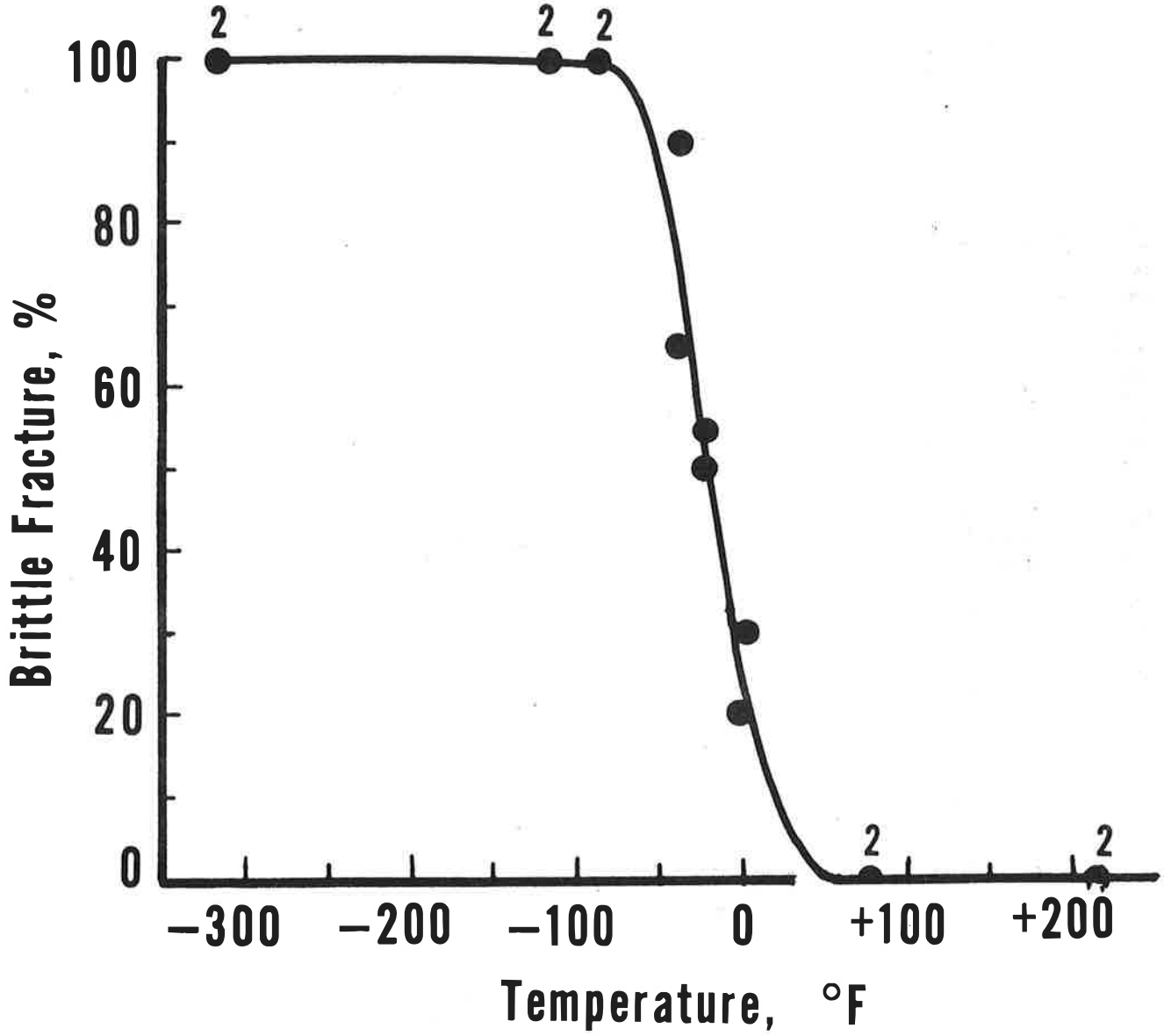

Figure 20. Effect of test temperature on the percentage of brittle fracture area of Group B1 impact specimens.

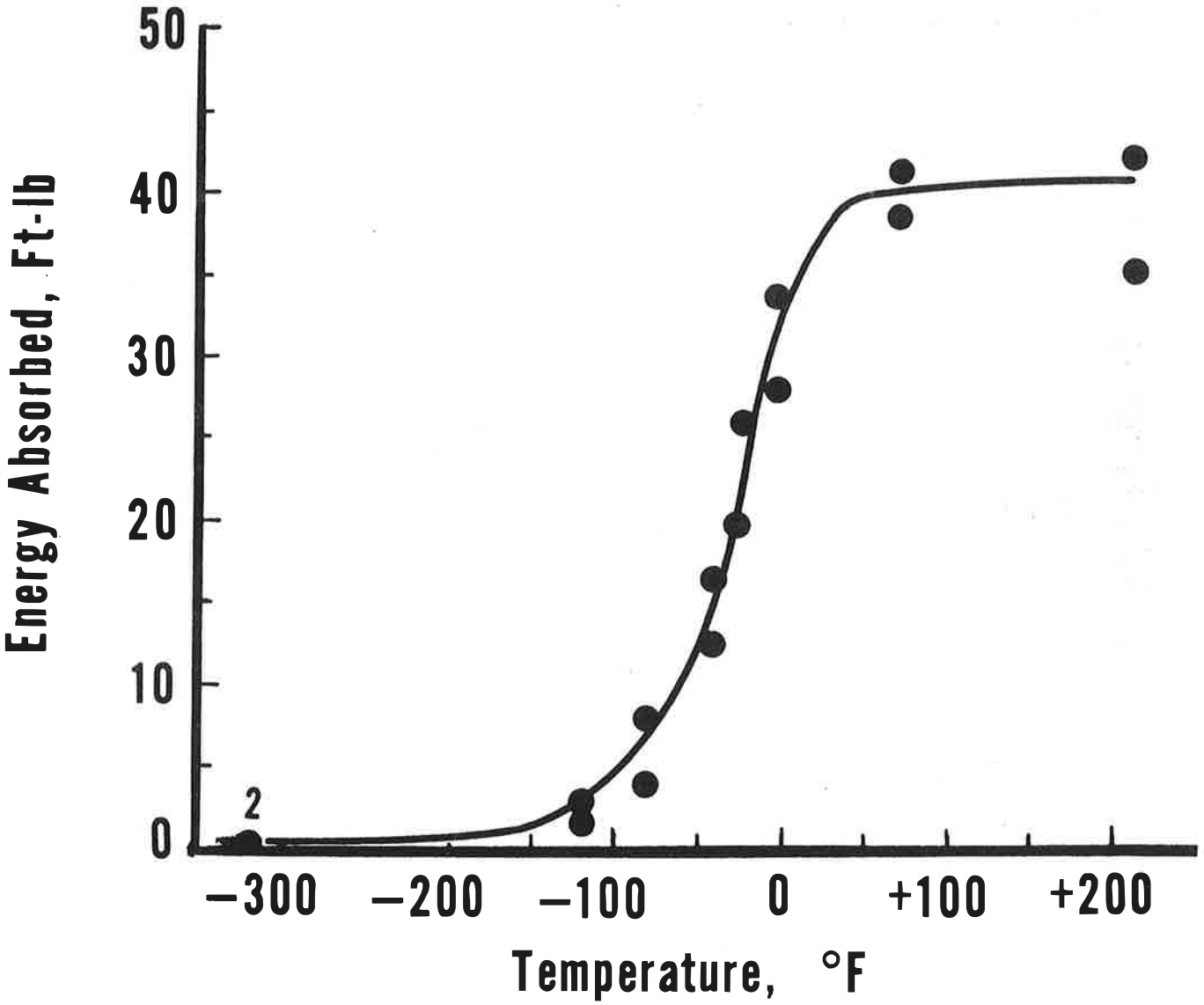

Figure 21. Effect of test temperature on the energy absorbed during fracture of Group B1 impact specimens.

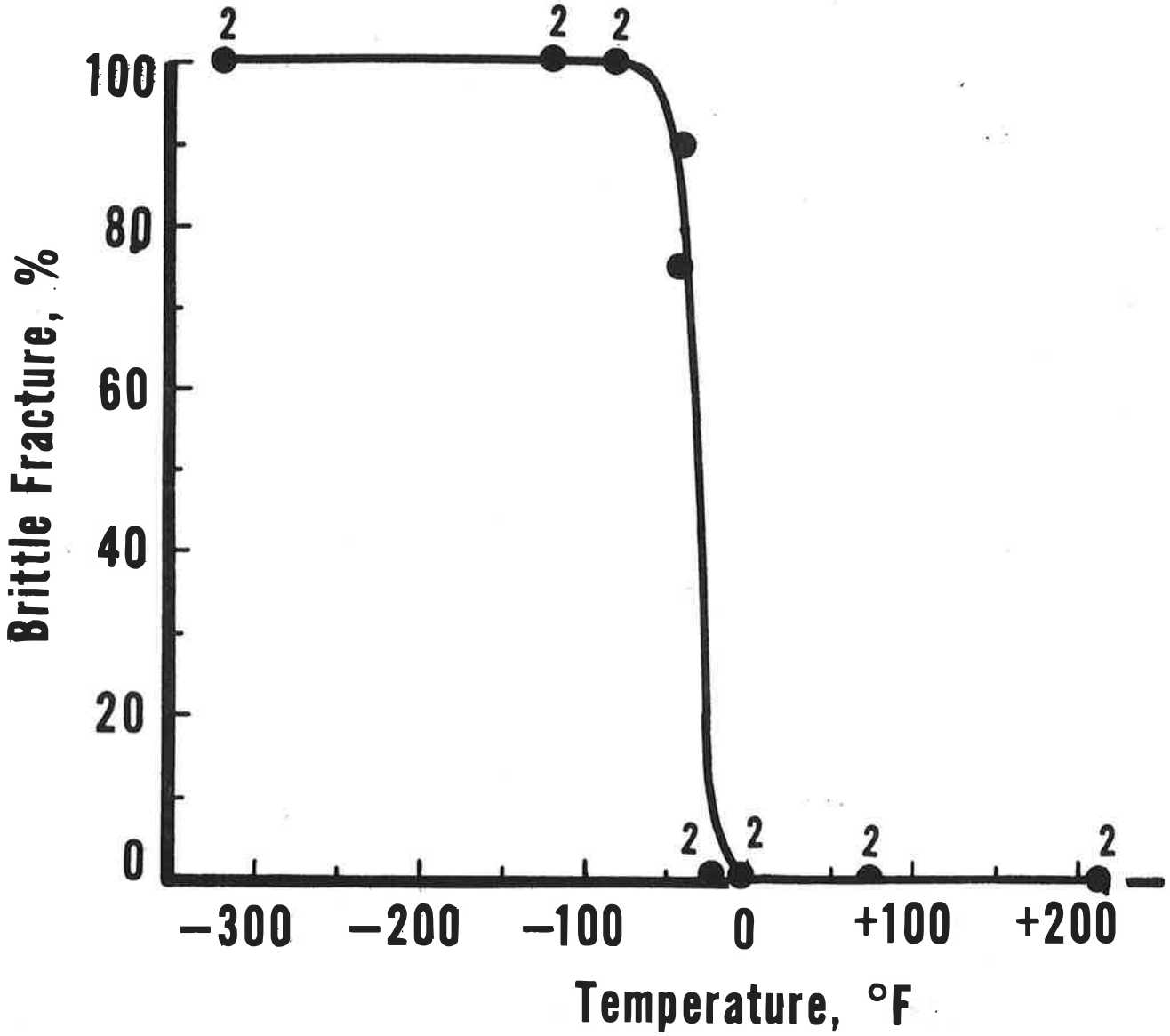

Figure 22. Effect of test temperature on the percentage of brittle fracture area of Group C1 impact specimens.

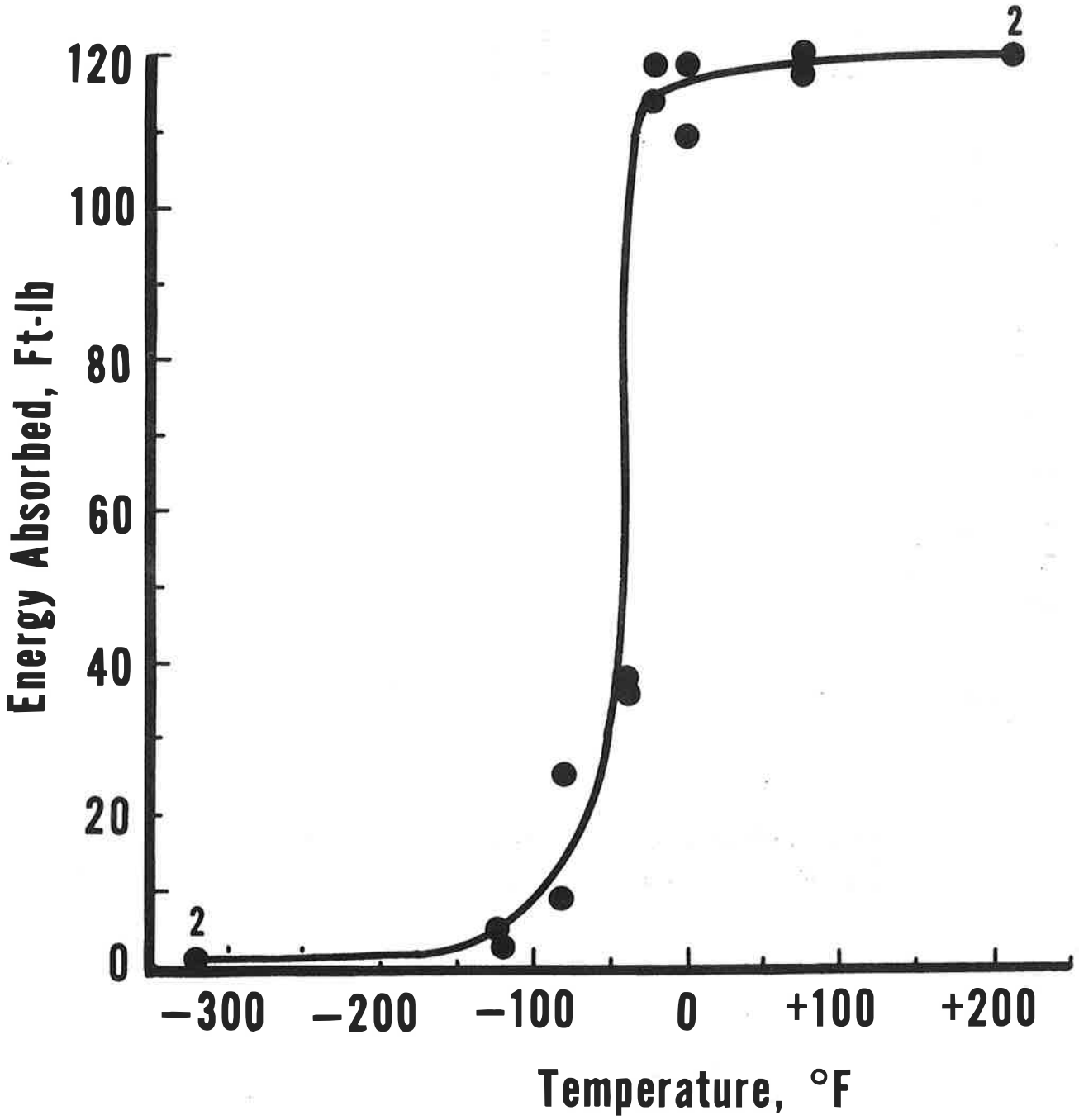

Figure 23. Effect of test temperature on the energy absorbed during fracture of Group C1 impact specimens.

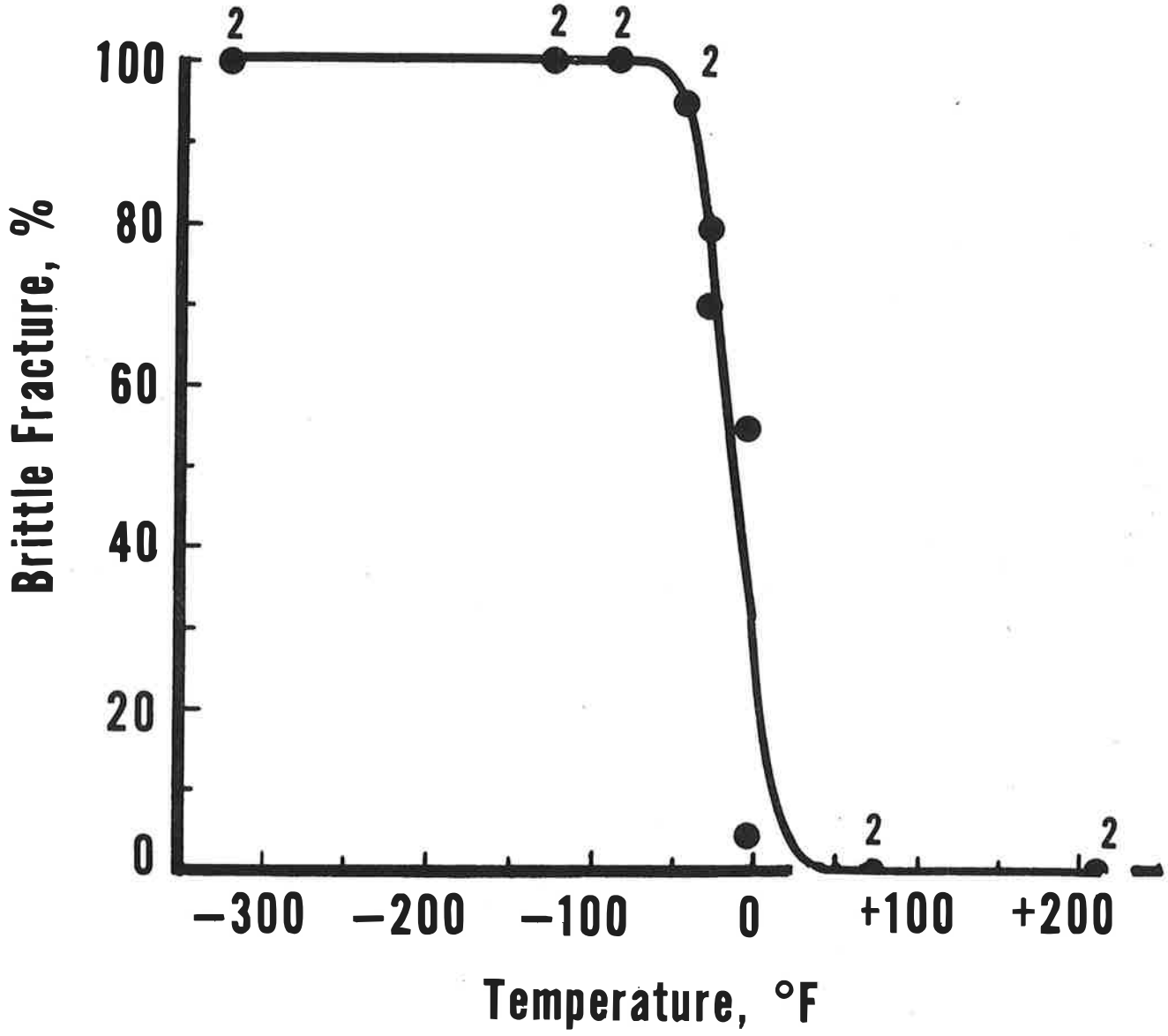

Figure 24. Effect of test temperature on the percentage of brittle fracture area of Group D1 impact specimens.

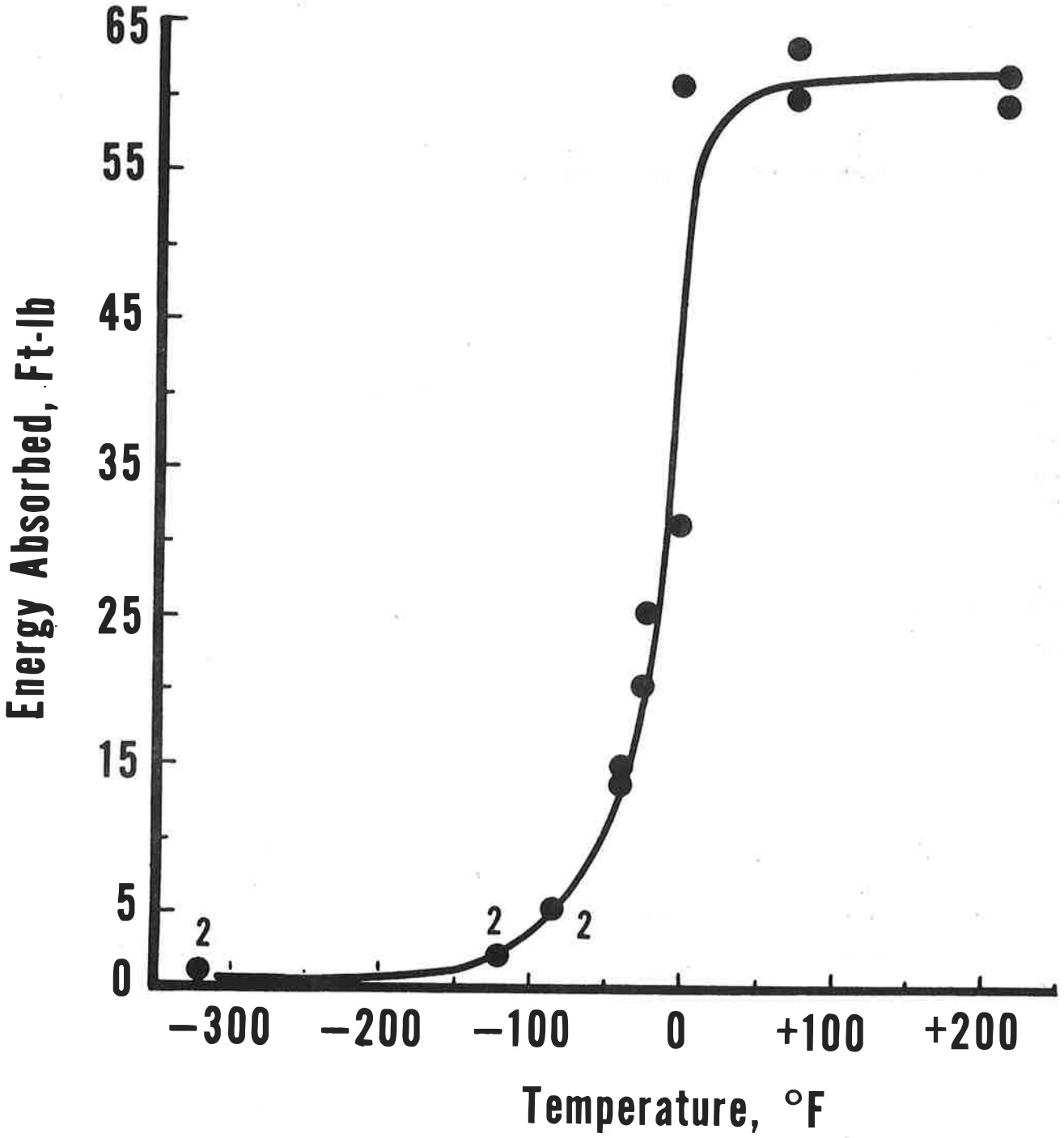

Figure 25. Effect of test temperature on the energy absorbed during fracture of Group D1 impact specimens.